

A Ratiometric Method for Johnson Noise Thermometry Using a Quantized Voltage Noise Source

S. W. Nam¹, S. P. Benz¹, J. M. Martinis¹, P. Dresselhaus¹, W. L. Tew², and
D. R. White³

¹National Institute of Standards and Technology, Boulder, CO, USA

²National Institute of Standards and Technology, Gaithersburg, MD, USA

³Measurement Standards Laboratory, Lower Hutt, New Zealand

Abstract. Johnson Noise Thermometry (JNT) involves the measurement of the statistical variance of a fluctuating voltage across a resistor in thermal equilibrium. Modern digital techniques make it now possible to perform many functions required for JNT in highly efficient and predictable ways. We describe the operational characteristics of a prototype JNT system which uses digital signal processing for filtering, real-time spectral cross-correlation for noise power measurement, and a digitally synthesized Quantized Voltage Noise Source (QVNS) as an AC voltage reference. The QVNS emulates noise with a constant spectral density that is stable, programmable, and calculable in terms of known parameters using digital synthesis techniques. Changes in analog gain are accounted for by alternating the inputs between the Johnson noise sensor and the QVNS. The Johnson noise power at a known temperature is first balanced with a synthesized noise power from the QVNS. The process is then repeated by balancing the noise power from the same resistor at an unknown temperature. When the two noise power ratios are combined, a thermodynamic temperature is derived using the ratio of the two QVNS spectral densities. We present preliminary results where the ratio between the gallium triple point and the water triple point is used to demonstrate the accuracy of the measurement system with a standard uncertainty of 0.04 %.

INTRODUCTION

Johnson Noise Thermometry (JNT) is a primary thermometry method in which the random voltage fluctuations in a conductor are measured to infer a thermodynamic temperature T [1]. In the classical limit of $hf \ll kT$, the spectral density S_T of the voltage noise power across a conductor is independent of frequency f and given by

$$S_T = 4kTR, \quad (1)$$

where R is the conductor resistance and k is the Boltzmann constant. The mean-square of the fluctuating Johnson noise voltage, V_T , in the frequency band between f_1 and f_2 is then given by

$$\overline{V_T^2} = \int_{f_1}^{f_2} S_T df, \quad (2)$$

which reduces to the familiar Nyquist formula $4kTR\Delta f$ for a constant (flat) spectral density. The mean-square

Johnson noise voltage $\overline{V_T^2}$ is the statistical variance of the distribution of the zero-mean time-series $v(t)$. This distribution is Gaussian for large samples.

The most successful JNT measurement technique developed to date is the switched-input noise-correlator pioneered by Brixy, *et al.* [2]. In the digital versions of this instrument, the noise from two parallel channels, x and y , are simultaneously sampled and Fourier transformed. The transformed voltage densities $v_x(f)$ and $v_y(f)$ are superpositions of extraneous channel dependent noise, v_{nx} and v_{ny} , and a common Johnson noise component v_T that is proportional to the temperature of interest. The extraneous noise in the two channels is uncorrelated, while the Johnson noise remains correlated such that when the cross-correlated spectral density, S_{xy} , is formed by the product

$$S_{xy} = v_x(f)v_y^*(f), \quad (3)$$

the spectral density of the Johnson noise alone, S_T , is recovered in the limit of large sample size.

Contribution of the National Institute of Standards and Technology, not subject to copyright

The conventional switched-input Digital Noise Correlator (DNC) alternates the inputs between a Johnson-noise reference voltage V_0 from a resistance $R(T_0)$ at a known reference temperature T_0 , and another Johnson noise source V_T , from a resistance $R(T)$ at an unknown temperature T . The switching removes the effects of drifts in the gain and bandwidth of the amplifiers and filters. The unknown temperature is then inferred as

$$T = \frac{\overline{V_T^2}}{\overline{V_0^2}} \frac{R(T_0)}{R(T)} T_0 \quad (4)$$

which requires only measurements of the resistance ratio and noise power ratio. In practice, the inherent non-linearity of the amplification process requires the input noise powers to be matched. This imposes a constraint on the resistance values given by the expression $R(T_0)T_0 = R(T)T$.

The conventional method has limitations due to the inevitable coupling of the DNC pre-amplifier input capacitance, transmission-line impedance, and source resistance [3]. These impedance couplings cause frequency dependent systematic errors in the measured noise power ratio. These errors arise due to the constraints on the RT product. There are insufficient design parameters available when the Johnson noise provides a dual function of both voltage and temperature reference. There are also difficulties in the conventional DNC systems in designing the bandpass filter using analog techniques.

The JNT measurement system described here is also a switched-input DNC and therefore similar to the conventional systems, but also incorporates new elements that are designed to address the limitations and difficulties found in the conventional methods [4]. First, the roles of the noise voltage reference and the reference temperature T_0 are separated by using a purely electronic voltage reference, the Quantized Voltage Noise Source (QVNS). The QVNS reference is based on Josephson pulse-quantization [5] and digital AC voltage waveform synthesis [6] that allows accurate AC voltages to be synthesized at the very small power levels necessary for JNT. The other main innovation of this system is the implementation of digital filtering in the DNC electronics. This feature allows for a stable and predictable bandwidth where all the filter parameters are programmable.

From a voltage metrology standpoint, the principle advantages to using the QVNS reference are: (1) The synthesized noise power is a programmable variable that can be matched to the Johnson noise power independent of any impedance matching constraints. (2) The QVNS output is highly stable, allowing a reference noise power ratio to be established at some arbitrary time that may be non-concurrent with another noise power ratio measured at the unknown temperature. (3) The QVNS may be used to check the linearity and frequency response of the measurement system and hence establish the degree to which the noise powers must be matched. (4) The QVNS voltage is calculable from knowledge of the digital synthesis algorithm, the clock frequency and fundamental constants. (5) The QVNS generates a pseudo-random noise, which is deterministic and so obeys slightly different statistics than does purely random Johnson noise. Hence, the statistical precision of measurements of the QVNS are slightly better than the Johnson noise for the same number of samples. [4]

From the standpoint of temperature metrology, the QVNS allows a ratiometric method for JNT that has not previously been available. The method involves the measurement of two different noise power ratios. One ratio is formed by matching the QVNS reference voltage V_{r,T_0} to the Johnson noise voltage V_0 at a known temperature T_0 . The other ratio is formed by matching a new QVNS reference voltage $V_{r,T}$ to the Johnson noise voltage V_T at the unknown temperature T . The DNC inputs are switched between V_T and V_r , to measure the ratio V_T^2/V_r^2 , which is near unity for every T measured. The temperature is then inferred from a modification of Equation (4):

$$T = \frac{\overline{V_T^2}}{\overline{V_{r,T}^2}} \frac{\overline{V_{r,T_0}^2}}{\overline{V_0^2}} \frac{S_{r,T}}{S_{r,T_0}} \frac{R(T_0)}{R(T)} T_0, \quad (5)$$

where the ratio $S_{r,T}/S_{r,T_0}$ is the calculated ratio of QVNS spectral densities based on the digital synthesis.

From an impedance standpoint, in this scheme it is necessary to know only the ratio of a single resistance at two different temperatures. Also, because both the QVNS and the Johnson noise resistor are measured twice, the effects of the unknown transfer functions of the different transmission lines are greatly reduced.

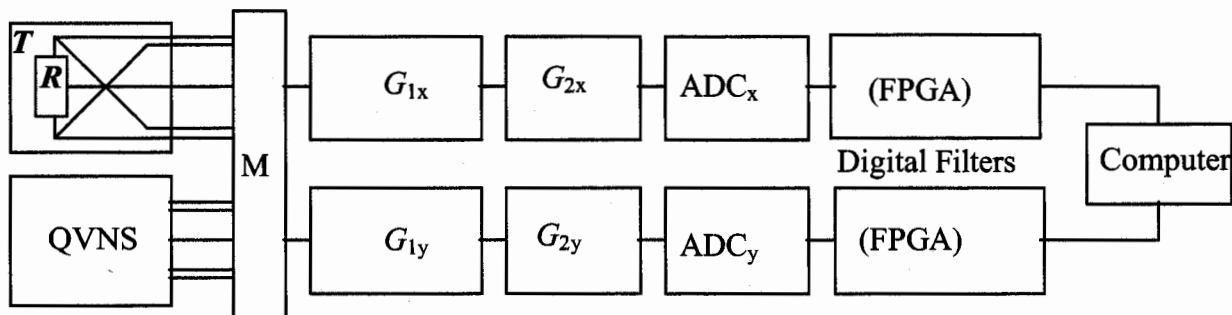


FIGURE 1. The measurement system block diagram. The two noise sources are Johnson noise from the sensing resistor R at a temperature T , and the QVNS synthesized source. These are connected to the multiplexer M , which routes signals to the two channels, which consist of the pre-amps with gains G_{1x} and G_{1y} , the anti-alias filters with gains G_{2x} and G_{2y} , the ADCs, and the digital filters (Field Programmable Gate Arrays) that are simultaneously sampled by the computer via fiber optic data links.

Normally, all the measured ratios can be held fairly close to unity, so the scaling of the temperature in Equation (5) can be accomplished almost entirely via the linearity of the QVNS synthesis of V_r . This is in contrast to the conventional technique where the scaling must be accomplished by the resistance ratio.

EXPERIMENTAL SYSTEM

A block diagram of the entire experimental system is shown in Figure 1. The system is a composite of three sub-systems: (1) the QVNS reference system; (2) the Johnson noise temperature probes and fixed-point cells; and (3) the DNC measurement system. While the three subsystems are each screened with conventional instrumentation enclosures, the laboratory environment has no special overall shielding for electromagnetic interference (EMI).

Quantized Voltage Noise Source

Josephson-based AC voltage sources are intrinsically accurate, Digital-to-Analog Converters (DAC) that can synthesize any AC waveform up to 10 MHz [6]. These AC voltage sources have been developed into pulse-driven, arbitrary-waveform synthesizers for a variety of applications in addition to the QVNS. In general, both the arbitrary waveform synthesizer and the QVNS produce voltage signals with calculable magnitudes based on the quantization of voltage pulses produced by an array of Josephson junctions. The quantization condition on voltage pulses $V(t)$ is $\int V(t)dt = \phi_0$, where ϕ_0 is a flux quantum, ($\phi_0 = h/2e$, h is Planck's constant and e is the electron charge). Knowledge of the number of pulses and their position in time is sufficient to precisely

determine the time-dependent voltage of any synthesized waveform. Thus, digital synthesis using perfectly quantized pulses enables the generation of waveforms with amplitudes that are dependent only on fundamental constants and a time standard [5].

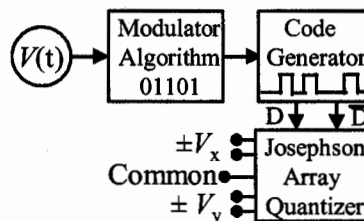


FIGURE 2. Block diagram of the QVNS. A desired analog pseudo-noise voltage waveform $V(t)$ is converted to a digital code by the modulator algorithm. Using this code, a two-level, 10 Gbit/s code generator drives two Josephson arrays using both Data and Data-complement channels. A common and two separate differential voltage taps, V_x and V_y , across the series-coupled arrays, are used for calibrating the DNC.

The basic method of noise synthesis used for JNT is illustrated in Figure 2. The required spectral densities of the noise voltages for the JNT are of order $1 \text{ nV}\cdot\text{Hz}^{-1/2}$. The QVNS is biased with unipolar pulses from a high-speed digital code generator. In response to these unipolar input pulses, the Josephson array quantizer likewise produces only unipolar output pulses of a single polarity. The use of both the digital pulse pattern D and its complement \bar{D} from the code generator allows the QVNS to source a differential output voltage with a symmetrically positioned common tap [7].

In practice, a pseudo-noise waveform is chosen consisting of a sequence of constant-amplitude harmonic tones with random relative phases. A binary digital pattern is created from this desired analog waveform using a delta-sigma modulator algorithm. The noise waveform is periodic because the digital

pattern is continuously circulated through the code generator's serial memory. The low-frequency limit and tone spacing of the waveform is given by $f_1 = f_s/M$, as set by the available pattern memory M and the clock frequency f_s . The current prototype system uses a 10 GHz clock but is limited to only 8 Mbit of memory, allowing only $f_1 \geq 1.2$ kHz. The rms voltage amplitude of each tone, V_{rms} , can be chosen to match the noise-voltage density of a resistor at any temperature, such that $V_{\text{rms}}^2 = 4kTRf_1$. Additional details on the QVNS biasing and operation are found in reference [7].

Temperature Sub-systems

The Johnson noise resistor is the sensing element in a shielded temperature probe. Most of the resistors tested have been three-terminal, metal-foil, surface-mount devices with a total resistance of 100 Ω and temperature coefficients of $< 10^{-5} \text{ K}^{-1}$. The noise signals are transmitted from the resistor via shielded twisted pairs with a center tap on the resistor tied to an inner shield. The measurement system does not apply any bias to the resistor other than the JFET gate current of < 0.1 pA. Consequently, the effect from $1/f$ noise in the resistor is negligible.

The temperature probes are equilibrated in either of two immersion-type fixed-point cells, a gallium triple point (Ga TP), and a water triple point (WTP). The cells have immersion depths of approximately 18 cm and 26 cm, respectively. Due to the high stem-conduction loss in the Johnson noise probes, there are still immersion errors, but these are no worse than 1 mK at full immersion. The difference between the plateau temperature of the Ga TP cell being used here and that of NIST reference cells is less than 0.1 mK when compared via a standard platinum resistance thermometer.

The two cell maintenance systems are commercial units optimized to minimize power requirements. The only exception being the power supplies, which are restricted to linear types in order to avoid EMI generally associated with any switching-type supply.

Digital Noise Correlator

The DNC electronics is composed of all the blocks to the right of (and including) the multiplex switching board M in Figure 1. All the signal-processing blocks are battery powered, with the exception of the computer. The analog gains G_{ij} are associated with the $j=x,y$ channels. The first stages are differential

common-source Junction Field Effect Transistor (JFET) pre-amps with bipolar bias transistors arranged as common-source cascodes according to the well-established designs of White and Zimmerman [3]. The role of the second-stage analog blocks ($i=2$) is to provide anti-alias filtering for the analog-to-digital converters (ADCs) above a 3 dB point of 2 MHz via a 4-pole low-pass Bessel filter. The equivalent input noise voltage of the amplifier chain is $1 \text{ nV}\cdot\text{Hz}^{-1/2}$. The ADCs sample 14 bits at rates of 50 MSample/s. The Field-Programmable Gate Arrays (FPGA) take these oversampled data streams from the ADCs and digitally implement a 22-bit, 8-pole Butterworth low-pass filter with a 3 dB point at 200 kHz. The digitally processed data is downsampled and transmitted at $f_p=2.083$ MSample/s through separate fiber-optic data links with a custom interface card in the computer's PCI bus.

The computer currently used is a 1.5 GHz dual-processor machine with 2 GByte of random access memory. The program that executes the streaming of data into memory must also process the raw data before writing to a hard disk volume. This processing consists of performing two 2^{21} point Fast Fourier Transforms (FFTs) for the two channels and then forming the two power spectra $S_{xx} = |v_x(f)|^2$ and $S_{yy} = |v_y(f)|^2$, and the cross-spectrum $S_{xy} = v_x(f)v_y^*(f)$. The three spectra are then successively accumulated with each new data sample. This entire process takes place in approximately one second. The same process must be repeated when the DNC switches to the other noise source, giving a total of six accumulated spectra stored in two different files.

PRELIMINARY RESULTS

Because of complexities in measuring the QVNS tones described in [9], the prototype system has been tested by comparing the Johnson noise at both 273.16 K and 302.916 K to a QVNS synthesized noise waveform with a voltage spectral density $S_r^{1/2} = 1.293 \text{ nV}\cdot\text{Hz}^{-1/2}$. This spectral density matches the Johnson noise in a 100 Ω probe at the Ga TP but is approximately 10 % higher than the Johnson noise at 273.16 K. The QVNS synthesized waveform consists of 1258 harmonic tones starting at $f_1=1.589$ kHz. The digital code was 6 291 456 bits long and each tone generated by the 8200-junction array had an amplitude of 51.549 nV, to produce $1.293 \text{ nV}\cdot\text{Hz}^{-1/2}$ in voltage noise density.

Figure 3 is a plot of the S_{xy} for the Johnson noise of the resistor in the Ga TP cell. The data in Figure 4

shows the measured S_{xy} for the synthesized noise waveform. Only the first 650 synthesized tones are captured in the 1 MHz measurement band ($f_p/2=1.0415$ MHz). Both spectra have 1 Hz resolution and are accumulated from 200 spectra from sampling for one second. The QVNS power spectrum in Figure 4 illustrates several imperfections. The presence of EMI at power line harmonics and video display harmonics is evident. In addition, the aliasing of tones above 1 MHz into bins adjacent to the synthesized tones can be seen rising from the filtered background above 300 kHz.

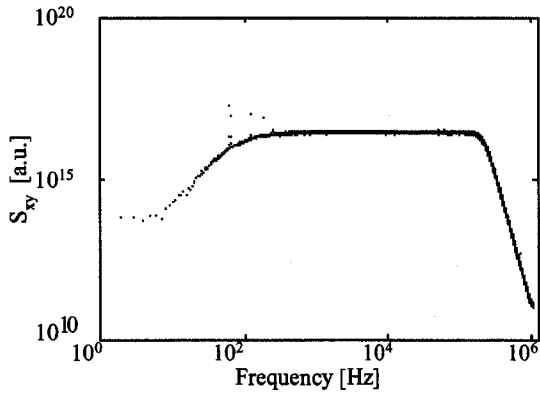


FIGURE 3. The average cross-power spectral density S_{xy} for a 100 Ω probe at 302.916 K.

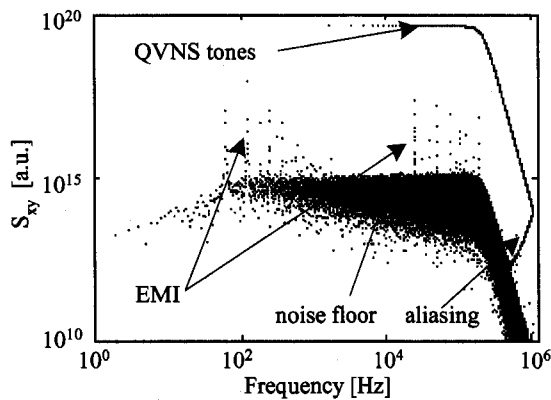


FIGURE 4. The average cross-power spectral density S_{xy} for the first 650 tones of a pseudo-noise pattern with a voltage noise density of $(S_r)^{1/2} = 1.293$ nV \cdot Hz $^{-1/2}$ (see text).

In order to ratio the Johnson noise spectra with the QVNS spectra, the Johnson noise must be corrected for aliasing and re-binned at each QVNS tone over a bandwidth equal to the frequency spacing of the QVNS tones (1.589 kHz). The resulting re-binned Johnson noise is then divided by the peak tone values in the QVNS spectra in an alternating sequence according to the switching of the inputs. For the Ga TP

the resulting noise power ratio spectrum is shown in the upper plot of Figure 5. A spectral average can in turn be made over all or some fraction of these bins. All 650 ratios can be used with equal weight under the assumption that the fraction of correlated to uncorrelated noise remains constant over those frequencies. In this case, the statistical precision of the data can be estimated by using the noise correlation bandwidth [8], $\Delta f_c \approx 235$ kHz for the filtering parameters used in the FPGAs.

The process of establishing a noise power ratio V_T^2 / V_r^2 for a single temperature T is repeated for the reference temperature T_0 , and a similar QVNS reference noise pattern of voltage V_{r,T_0} . In normal operation V_{r,T_0} would be synthesized with tone amplitudes that match the Johnson noise power at T_0 . In the data shown for the WTP on the lower trace of Figure 5, however, the same QVNS reference spectrum of $S_r^{1/2} = 1.293$ nV \cdot Hz $^{-1/2}$ was used. In this test case the measured power ratio was approximately 0.90, so the DNC provided all of the scaling rather than the QVNS. In either case, these two ratios can still be combined according to Equation (5), or the individual ratios can stand alone as part of an absolute measurement of temperature given the calculable aspect of the QVNS. We present a separate treatment of this latter approach elsewhere [9].

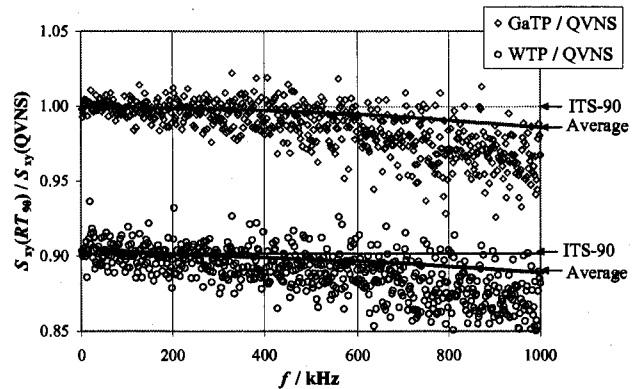


FIGURE 5. The 650 bin noise power ratio spectra for the Ga TP and WTP. The theoretical ratios according to ITS-90 assignments and integrated spectral averages are also shown.

The two power-ratio spectra of Figure 5 both exhibit a frequency dependence that deviates from a constant spectral density by approximately 3% over the measurement band. This is a systematic difference in the DNC gain spectral response between the QVNS synthesized noise and the temperature probe Johnson noise, possibly due to transmission-line effects [4].

A summary of the preliminary data is given in Table 1. The average noise power ratios are obtained by integrating the ratio spectra from f_l through f_u . The fourth column contains the predicted ratios based on the theory, ITS-90 assignments, and calculation of the QVNS synthesized code (Equation (5) in the case of the last two rows). The uncertainties are estimates based on a combination of statistical components and a 0.01 % Type B component in each power spectrum to account for EMI.

For the V_{GaTP}^2/V_r^2 data, the noise power densities were matched to within 0.03 %, and the measured power ratio given in the first row of Table 1 agrees within the uncertainty with the theory prediction for the first 100 kHz bandwidth. When the integration is carried out to the Nyquist limit $f_u = f_p/2$ however, the measured ratio deviates from the theory by 1.5 %. In contrast, the V_{WTP}^2/V_r^2 data were taken with the noise power densities 10 % out of balance, and the measured ratio over 100 kHz is accurate to only 0.15 %. This inaccuracy is generally expected to occur due to non-linearity in the DNC amplifier channels. Despite this non-linearity error, the cumulative spectral averages over the entire measurement band ($f_p/2$) of the two simple ratios are sufficiently similar that the frequency effect is largely canceled when the ratios are combined to form $V_{\text{GaTP}}^2/V_{\text{WTP}}^2$ according to Equation (5). In this case the agreement with theory is again well within the uncertainty. The last row in Table 1 recasts this combined power ratio as a temperature ratio via Equation (5). The temperature ratio over the 100 kHz band is offset from the ITS-90 value by 3σ , but the agreement is much better when integrated to 1.03 MHz.

TABLE 1. JNT data summary for Ga TP and WTP.

Ratios	average, $f_u=100$ kHz	average, $f_u=1.03$ MHz	Theory (ITS-90)
V_{GaTP}^2/V_r^2	0.99967(41)	0.98531(25)	0.99978
V_{WTP}^2/V_r^2	0.90295(38)	0.88837(23)	0.90148
$V_{\text{GaTP}}^2/V_{\text{WTP}}^2$	1.10711(65)	1.10911(40)	1.10904
$T_{\text{GaTP}}/T_{\text{WTP}}$	1.10700(65)	1.10901(41)	1.10893

In order to understand the errors in the temperature measurement, various effects on the noise power synthesis and measured ratios have been investigated: (a) the degree of accidental coupling in the Josephson Array Quantizer between the input microwave patterns and the output voltage waveforms; (b) the coupling of the large out-of-band ($f > 10$ MHz) power on the

QVNS outputs which is a consequence of the synthesis method [7], a small fraction of which can be mixed into the lower frequency measurement band when the QVNS output is amplified in the JFETs of the DNC [9]; (c) loading effects from filter and cable capacitance, which depend on which noise source is being sampled; and (d) EMI coupling and grounding.

While these preliminary results are encouraging, we expect the accuracy of the ratiometric method to further improve using a fully balanced set of data. In addition, we will focus on understanding the difference in frequency response of the QVNS and the Johnson noise. A custom-built digital code generator with 1 Gbit of re-circulating memory is being developed for the QVNS. This will allow a 10 Hz line spacing in the QVNS reference spectra for more detailed evaluations of the frequency dependence and other effects of non-linearity in the DNC.

ACKNOWLEDGMENTS

We wish to acknowledge Fred Walls of Total Frequency, Inc., for helpful discussions on electronics, Greg Strouse of NIST for measurements of the Ga TP cell, Norm Bergren of NIST for assistance in setting up facilities for our measurements, and Charlie Burroughs of NIST for construction of the 4K probe.

REFERENCES

- White, D. R., *et al.*, *Metrologia* **33**, 325-335 (1996).
- Brixy, H., *et al.*, in: *Temperature: Its Measurement and Control in Science and Industry*, Vol. 6, edited by J. F. Schooley, American Institute of Physics, New York, 1992, 993-996.
- White, D. R., and Zimmermann, E., *Metrologia* **37**, 11-23 (2000).
- Benz, S. P., *et al.*, in: *Proceedings of TEMPMEKO 2001*, edited by B. Fellmuth, J. Seidel, and G. Scholz, VDE Verlag, 2002, Berlin, pp. 37-44.
- Hamilton, C. A., Burroughs, C. J., and Kautz, R. L., *IEEE Trans. Instrum. Meas.* **IM-44**, 223-225 (1995).
- Benz, S. P., *et al.*, *IEEE Trans. Instrum. Meas.* **IM-50**, 181-184 (April 2001).
- Benz, S. P., *et al.*, *IEEE Trans. Instrum. Meas.* **IM-52**, in press (April 2003).
- White, D. R., *IEEE Tran. Instr. Meas.* **IM-38**, 1036-1043 (1989).
- Nam, S. W., *et al.* *IEEE Trans. Instrum. Meas.* **IM-52**, in press (April 2003).